Journal of Alloys and Compounds, 213/214 (1994) 173–177
JALCOM 4090

Thermodynamic properties and multiphase diffusion paths of the ternary system U–Zr–N

Toru Ogawa and Mitsuo Akabori
Japan Atomic Energy Research Institute, Tokai-mura, Naka-gun, Ibaraki-ken 319-11 (Japan)

Abstract

Recent studies of the nuclear transmutation of actinide wastes have revived a general interest in actinide alloys and nitrides. The thermodynamic properties of U–Zr–N alloys are described with a sublattice formalism. The calculated equilibria in the ternary system were compared with recent experiments on the reactions of U–Zr alloys with nitrogen. Multiphase diffusion paths in the reactions were readily explained by a stability diagram calculated with the present model. It was also shown that the previous models of U–Zr and Zr–N alloys are consistent with each other and that the thermodynamic properties of U–Zr alloys at about 1000 K, experimental data on which have been lacking, are reasonably represented by the model.

1. Introduction

Recent studies on the nuclear transmutation of actinide wastes have revived a general interest in actinide alloys and nitrides. Alloy and nitride fuels are characterized by higher metal densities, which could give harder neutron spectra appropriate for efficient burning of waste actinides. In analysing the behaviour of these fuels, we need to know the thermodynamic properties of multicomponent systems containing actinide and transition metals. Among the alloy fuels containing transuranium elements, U–Pu–Zr-based alloys have been extensively studied [1–3]. There are other concepts of alloy fuels where minor actinides: Np, Am, Cm etc. (MA) themselves are major components [4], but the database of the transuranium alloy systems is still inadequate. The existing data on the alloying behaviour among U, Np, Pu and Am have been reviewed and compared with predictions made using the Brewer theory [5]. More recently phase equilibria in selected Np binary systems have been investigated [6–8].

The U–Zr binary system is one of the most extensively investigated alloy systems of uranium and accurate knowledge of this system should provide a basis to understand the behaviour of other systems such as Np–Zr. However, accurate measurements of the thermodynamic properties of U–Zr alloys are difficult owing to the high reactivities of the components. In this study, the behaviour of the ternary system U–Zr–N is analysed and compared with experimental observations on the reactions of U–Zr alloys with nitrogen by Akabori *et al.* [9]. The reason for studying this particular system is threefold.

(1) From the equilibria in the U–Zr–N system one could estimate the phase stability of U–Zr alloys.

(2) A Zr-rich layer has been observed near the surface of U–Pu–Zr fuels, which retards molten phase formation at the fuel–cladding interface [10]. Formation of the Zr-rich layer seems to be related to the availability of impurity nitrogen.

(3) It has been claimed that the addition of ZrN to nitride fuels prevents U-rich liquid phase formation at very high temperatures [11].

2. Analysis

The constitution of U–Zr alloys is relatively well established [12, 13]. Continuous b.c.c. solid solutions (γ-U, β-Zr) exist at high temperatures below the solidus. There is a miscibility gap whose critical point is $T \approx 995$ K at the Zr atomic fraction $X_{Zr} \approx 0.3$, indicating a positive deviation from the ideal mixing behaviour. However, there is an intermediate phase δ below about 890 K at $X_{Zr} \approx 0.7$, the presence of which indicates a negative interaction between U and Zr around this composition. Uranium vapour pressures over the alloys at about 1873 K [14, 15] agree with the model by Ogawa and Iwai [16]. The thermodynamic models of Leibowitz *et al.* [17] and Ogawa and Iwai [16] differ at such high temperatures, but agree very well with each other at about 1000 K. Both models rely largely on the same phase diagram information. However, reliable thermodynamic data below 1000 K are needed.

SSDI 0925-8388(94)04090-Q

TABLE 1. Summary of known ternary behaviour of terminal solution phases

Phase	Behaviour
α-U	Limited solubility of Zr and N
β-U	Limited solubility of Zr and N
b.c.c. (γ-U, β-Zr)	Limited solubility of N below 1200 K
h.c.p. (α-Zr)	Limited solubility of U; significant solubility of N

The thermodynamic properties of U–Zr–N alloys can be represented by a sublattice formalism [18, 19] in which each alloy phase is regarded as consisting of metal and non-metal sublattices. The metal sublattice is filled with a mixture of U and Zr, the non-metal sublattice with a mixture of N and its vacancy (V). The Gibbs free energy of formation of a Φ phase alloy is then

$$\Delta G_f^\circ(\Phi) = Y_U Y_V \Delta G_f^\circ(\Phi\text{-U}) + Y_{Zr} Y_V \Delta G_f^\circ(\Phi\text{-Zr}) + Y_U Y_N \Delta G_f^\circ(\Phi\text{-UN}) + Y_{Zr} Y_N \Delta G_f^\circ(\Phi\text{-ZrN}) - T\Delta S_{ideal} + \Delta G^E(\Phi) \quad (1)$$

Y is the site occupation fraction:

$$Y_i^A = \frac{X_i^A}{\sum_i X_i^A} \quad (2)$$

where X_i^A is the atomic fraction of component i which resides on sublattice A. ΔS_{ideal} is the ideal entropy of mixing:

$$\Delta S_{ideal} = -R \sum_{A=1}^{2} \sum_{i=1}^{2} Y_i^A \ln Y_i^A \quad (3)$$

ΔG^E is the excess free energy of mixing:

$$\Delta G^E(\Phi) = Y_U \Omega_{U(N,V)} Y_N Y_V + Y_{Zr} \Omega_{Zr(N,V)} Y_N Y_V + Y_N \Omega_{(U,Zr)N} Y_U Y_{Zr} + Y_V \Omega_{(U,Zr)} Y_U Y_{Zr} \quad (4)$$

where $\Omega_{U(N,V)}$ is the binary interaction parameter between N and V on the non-metal sublattice when the metal sublattice is filled with U, $\Omega_{(U,Zr)N}$ is that between U and Zr on the metal sublattice when the non-metal sublattice is filled with N, and so on. The interaction parameters follow the Redlich–Kister formulation:

$$\Omega_{ij} = \sum_{p=1} \Omega_p (Y_i - Y_j)^{p-1} \quad (5)$$

where Ω_p is a polynomial coefficient which can be a function of temperature.

The relevant binary interaction parameters were taken from our previous studies and the literature: U–Zr [16], U–N [19], Zr–N [20] and UN–ZrN [21]. Some binary parameters are lacking, particularly for the terminal solution phases with the nitrogen addition. Appropriate parameters were assumed in such cases. For instance, $\Omega_{U(N,V)}$ (liquid alloys) [19] is used for phases other than f.c.c. Observations on the ternary behaviour of these phases are summarized in Table 1, which suggests that the errors in the assumed interaction parameters have insignificant effects on the calculated equilibria.

Generally the b.c.c. lattice of a transition metal is destabilized with respect to the h.c.p. and f.c.c. lattices by the addition of nitrogen. Crystallographic aspects of nitrogen incorporation into the b.c.c. lattice and a resulting ω-like local lattice distortion are discussed in ref. 19. The ω phase is a metastable phase of Zr-based alloys; rather minor displacements of (111) planes of the b.c.c. lattice result in the ω structure [22]. The

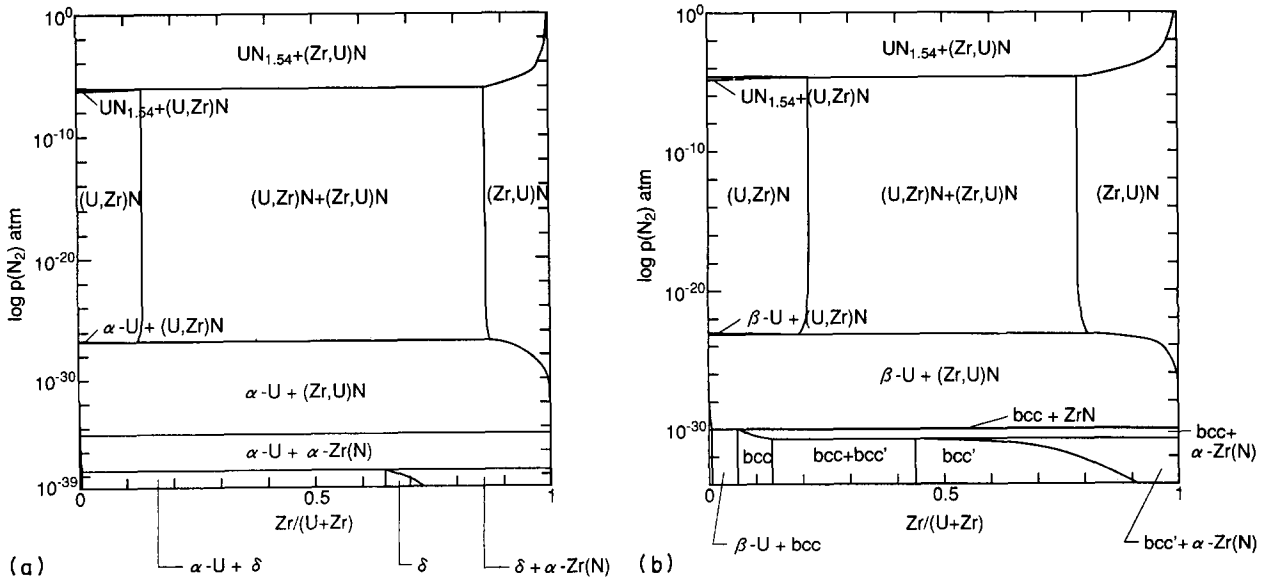

Fig. 1. Ternary equilibria as a function of $p(N_2)$ at (a) 873 K and (b) 973 K.

destabilization of the b.c.c. lattice is implicit in the N–V interaction parameters and lattice stability parameters of the b.c.c. and h.p.c. phases. The same N–V interaction parameters as those for the b.c.c. phase were assumed for δ, since the structure of δ appears to be closely related to that of ω [13, 23].

The solubility of Zr in U_2N_3 is assumed to be negligible; the phase is regarded as an invariant phase, $UN_{1.54}$ [24]. The equilibria were computed with a Gibbs free-energy minimizer, CHEMSAGE [25].

3. Results and discussion

3.1. Ternary isotherms

Calculated ternary isotherms are shown in Figs. 1 and 2. Two types of plots are adopted. Figure 1 shows how the stable phases change with the N_2 partial pressure $p(N_2)$. With increasing $p(N_2)$ δ decomposes into α-Zr(N) and α-U (Fig. 1(a)) and the b.c.c. solutions decompose into α-Zr(N) and a U-rich alloy (Fig. 1(b)). It is also shown that the homogeneity range of δ is a very sensitive function of nitrogen contamination. Thus the experimentally observed destabilization of δ and b.c.c. with nitrogen addition [9, 26] is correctly reproduced. With further increase in $p(N_2)$ h.c.p. α-Zr(N) is replaced by f.c.c. ZrN; U-rich alloys are replaced by UN and then U_2N_3.

In Fig. 2 the phase fields are plotted against the nitrogen content $Y_N = N/(U+Zr)$. The nitrogen solubility in α-Zr is large: $Y_N = N/Zr \approx 0.31$ or $X_N \approx 0.24$ at 973 K. The predicted U solubility in ZrN is a function of $p(N_2)$: it is very small in a sufficiently hyposto-

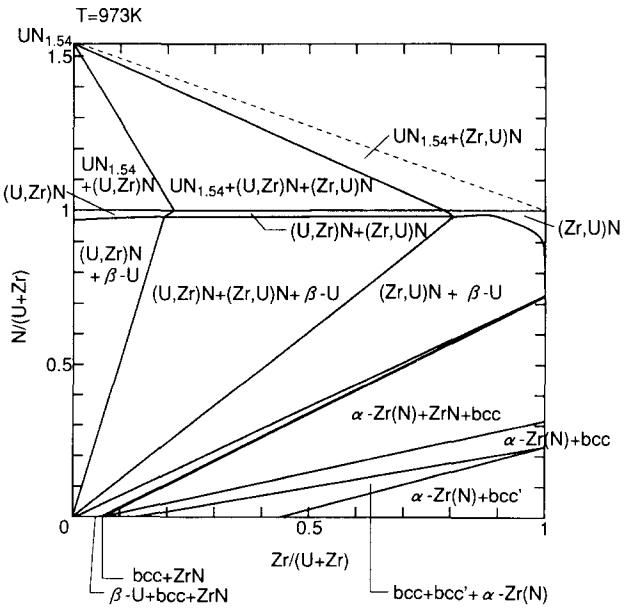

Fig. 2. Ternary isotherm at 973 K as a function of Zr/(U+Zr) and N/(U+Zr).

ichiometric ZrN_{1+x} (lower $p(N_2)$), but significantly large near the exact stoichiometry (higher $p(N_2)$).

3.2. Multiphase diffusion paths and stability diagram

The reaction layers on a $U_{0.5}Zr_{0.5}$ ingot at 973 K were [9]

U_2N_3/(Zr, U)N/α-Zr(N)($X_U \approx 0.001$, $X_N \approx 0.21$)/γ-U($X_{Zr} \approx 0.12$)/matrix

The U_2N_3 layer was barely recognized by electron probe microanalysis (EPMA). The thickness of the (Zr, U)N layer was about one-third of that of α-Zr(N). The compositions given in parentheses are the averages across each layer and vary only moderately. It is noted that the compositions of the α-Zr(N) layer, $Zr_{\sim 0.79}N_{\sim 0.21}$ ($Y_N = N/Zr \approx 0.27$), and the γ-U layer, $U_{\sim 0.79}Zr_{\sim 0.12}$, are along a tie-line of Fig. 2. Figure 3 shows the activities a in the Zr–N [19] and U–Zr alloys at 973 K. Hence

a(Zr) in α-Zr(N) $\approx a$(Zr) in (γ-U, β-Zr) ≈ 0.65

at the layer interface with an allowance for the experimental errors of EPMA. Thus the thermodynamic models of the U–Zr [16] and Zr–N [20] alloys are consistent with each other.

The reaction layer structure can be more readily discussed with the kind of stability diagram shown in Fig. 4, where the phase fields are plotted against a(Zr) and a(U). The $p(N_2)$ contours are shown by dashed lines. The fringe at zero N_2 partial pressure gives the isotherm of the U–Zr binary system. The diagram is a two-dimensional projection of the minimum free-energy (G_{min}) surface of the ternary system or it could also be regarded as a contour map of the G_{min} surface.

The reaction is considered to proceed along the nitrogen pressure gradient, since the interstitial nitrogen is the most mobile species of the system. Diffusion coefficients for relevant phases are found in refs. 27–29. The multiphase diffusion path would therefore run somewhere near the line connecting a point on the zero $p(N_2)$ fringe, which represents an original nitrogen-free alloy, and a point at the lower left corner, which is in the U_2N_3 ($UN_{1.54}$) field. The alloy compositions in the experiments by Akabori *et al.* [9] are on either side of the b.c.c. miscibility gap, which is the point MG in Fig. 4(b). The general layer sequence would be

U_2N_3/(Zr, U)N/α-Zr(N)/matrix

which agrees with the experimentally observed sequence.

For the $U_{0.5}Zr_{0.5}$ alloy at 973 K, which lies on the close right of the point MG in Fig. 4(b), the excess uranium due to the formation of (Zr, U)N and α-

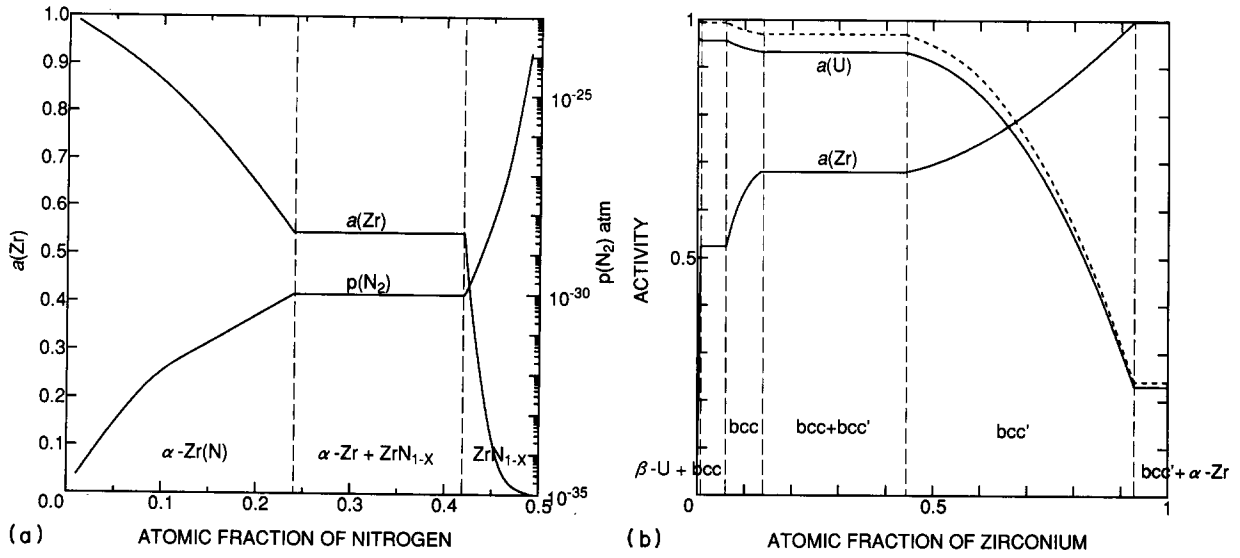

Fig. 3. Activities in (a) Zr–N [19] and (b) U–Zr alloys at 973 K: —— a(Zr), h.c.p. Zr; ——, a(U), b.c.c. U; – – –, a(U), β-U.

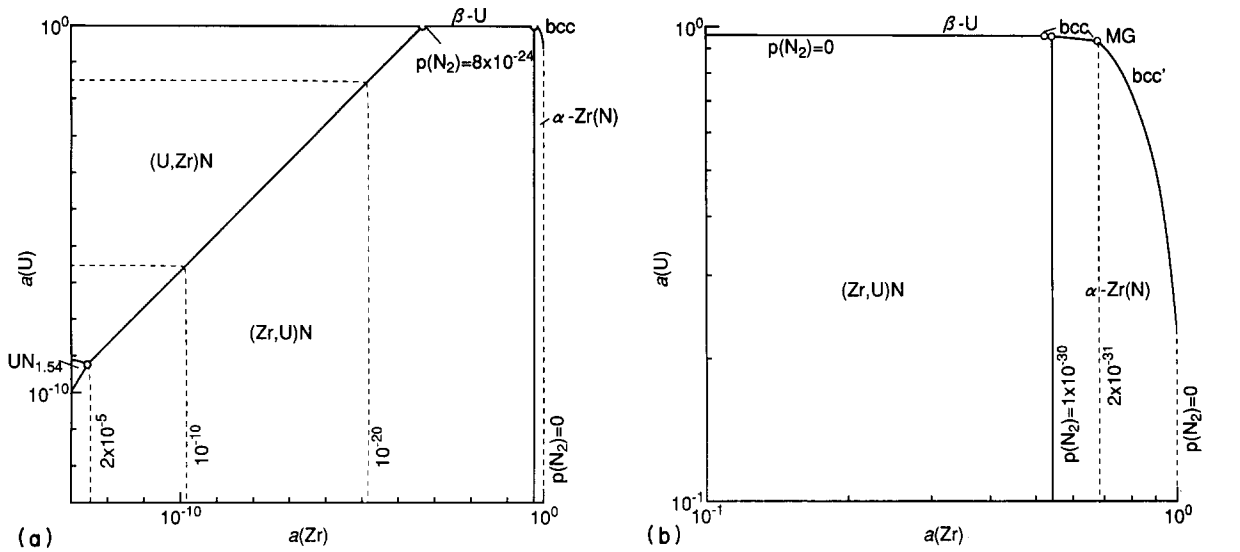

Fig. 4. Stability diagram or contour map of minimum free-energy surface of U–Zr–N alloys at 973 K; the upper right corner of (a) is enlarged in (b): – – –, $p(N_2)$ (atm); O, triple point; MG, b.c.c. miscibility map.

Zr(N) layers would either segregate or form another layer as a series of U-rich b.c.c. solutions. The excess uranium cannot be effectively removed to the surface to form U_2N_3, since (Zr, U)N acts as a diffusion barrier. Hence the layer sequence agrees with the experimentally observed one. It is noted that the $p(N_2)$ contour runs nearly parallel to that of a(Zr) in the (Z, U)N and α-Zr(N) fields in Fig. 4. The layer sequence gives a slight maximum in a(U) on crossing the point MG, while both zirconium and nitrogen migrate down their activities. An activity maximum and minimum of a component along the diffusion path can occur in a multicomponent system [30].

Hofman *et al.* [10] heated a $U_{0.61}Pu_{0.16}Zr_{0.23}$ ingot in contact with a ferritic steel at 973 K for 300 h and found the formation of Zr-rich layer a few microns thick which contained nitrogen almost to its solubility limit. This layer acted as an effective diffusion barrier to the metal atoms and prevented molten phase formation by the reaction of actinides with Fe and Ni at higher temperatures. Under their experimental conditions $p(N_2)$ would have been too low for U_2N_3 to be formed. The mononitride layer, which should be much thinner than the α-Zr(N) layer, would have been indistinguishable. The reaction layer structure is thus consistent with the present prediction.

References

1 Y.I. Chang and C.E. Till, in *LMR: a Decade of LMR Progress and Promise,* American Nuclear Society, La Grange Park, IL, 1991, pp. 129–137.
2 C.L. Trybus, S.P. Henslee and J.E. Sanecki, *ANS Trans., 66* (1992) 183.
3 T. Inoue, M. Kurata, L. Koch, J.C. Spirlet, C.T. Walker and C. Sari, *ANS Trans., 64* (1991) 552.
4 T. Mukaiyama, H. Takano, T. Takizuka, T. Ogawa, H. Yoshida and Y. Gunji, *ANS Trans., 64* (1991) 548.
5 T. Ogawa, *J. Alloys Comp., 194* (1993) 1.
6 R.G. Haire and J.K. Gibson, *J. Nucl. Mater., 195* (1992) 156.
7 J.K. Gibson and R.G. Haire, *J. Nucl. Mater., 201* (1993) 225.
8 J.K. Gibson, R.G. Haire and M.M. Gensini, paper presented at *Actinides-93, Santa Fe, NM, 1993.*
9 M. Akabori, A. Itoh, T. Ogawa and M. Ugajin, *J. Alloys Comp., 213/214* (1994) 366.
10 G.L. Hofman, A.G. Hins, D.L. Porter, L. Leibowitz and E.L. Wood, *Argonne National Laboratory Rep. Conf-860931-6,* 1986.
11 R.A. Potter and J.L. Scott, *US Patent Doc. 4,059,539A,* 1977.
12 R.I. Sheldon and D.E. Peterson, in T.B. Massalski, J.L. Murray, L.H. Bennett, H. Baker and L. Kacprzak (eds.), *Binary Alloy Phase Diagrams,* Vol. 2, American Society for Metals, Metals Park, OH, 1986, pp. 2150–2151.
13 M. Akabori, A. Itoh, T. Ogawa, F. Kobayashi and Y. Suzuki, *J. Nucl. Mater., 188* (1992) 249.
14 M. Kanno, M. Yamawaki, T. Koyama and N. Morioka, *J. Nucl. Mater., 154* (1988) 154.
15 A. Maeda, Y. Suzuki and T. Ohmichi, *J. Alloys Comp., 179* (1992) L21.
16 T. Ogawa and T. Iwai, *J. Less-Common Met., 170* (1991) 101.
17 L. Leibowitz, R.A. Blomquist and A.D. Pelton, *J. Nucl. Mater., 167* (1989) 76.
18 B. Sundman and J. Agren, *J. Phys. Chem. Solids, 42* (1981) 297.
19 T. Ogawa, *J. Nucl. Mater., 201* (1993) 284.
20 T. Ogawa, *J. Alloys Comp., 203* (1994) 221.
21 H. Holleck and T. Ishii, *Kernforschungszentrum Karlsruhe, Rep. KFK 1754,* 1973.
22 B.A. Hatt and J.A. Roberts, *Acta Metall., 8* (1960) 575.
23 E.R. Boyko, *Acta Crystallogr., 10* (1957) 712.
24 H. Tagawa, *J. Nucl. Mater., 51* (1974) 78.
25 G. Eriksson and K. Hack, *Metall. Trans. B, 21* (1990) 1013.
26 F.A. Rough, A.E. Austin, A.A. Bauer and J.R. Doig, *Battelle Memorial Institute Rep. BMI-1092,* 1956.
27 A.D. Le Claire, in H. Mehr (ed.), *Landolt-Börnstein Numerical Data and Functional Relationships in Science and Technology, New Series,* Vol. 26, *Diffusion in Solid Metals and Alloys,* Springer, Berlin, 1990, pp. 471–503.
28 A.D. King, G.M. Hood and R.A. Hold, *J. Nucl. Mater., 185* (1991) 174.
29 Hj. Matzke, *J. Chem. Soc., Faraday Trans., 86* (1990) 1243.
30 M.A. Dayananda, in M.A. Dayananda and G.E. Murch (eds.), *Diffusion in Solids: Recent Developments,* Metallurgical Society, Warrendale, PA, 1985, pp. 195–230.